Published in final edited form as:

Free Radic Biol Med. 2019 April ; 134: 268–281. doi:10.1016/j.freeradbiomed.2018.12.031.

Improving mitochondrial function with SS-31 reverses age-related redox stress and improves exercise tolerance in aged mice

Matthew D. Campbell[1], **Jicheng Duan**[6], **Ashton T. Samuelson**[1], **Matthew J. Gaffrey**[6], **Gennifer E. Merrihew**[2], **Jarrett D. Egertson**[2], **Lu Wang**[3], **Theo K. Bammler**[3], **Ronald J. Moore**[6], **Collin C. White**[3], **Terrance J. Kavanagh**[3], **Joachim G. Voss**[5,7], **Hazel H. Szeto**[8], **Peter S. Rabinovitch**[4], **Michael J. MacCoss**[2], **Wei-Jun Qian**[5], and **David J. Marcinek**[1]

[1]Department of Radiology, University of Washington, Seattle, WA

[2]Department of Genome Sciences, University of Washington, Seattle, WA

[3]Department of Environmental and Occupational Health Sciences, University of Washington, Seattle, WA

[4]Department of Pathology, University of Washington, Seattle, WA

[5]School of Nursing, University of Washington, Seattle, WA, USA

[6]Biological Sciences Division, Pacific Northwest National Laboratory, Richland, WA, USA

[7]Joachim Voss currently with Frances Payne Bolton School of Nursing, Case Western Reserve University, Cleveland, OH, USA

[8]Social Profit Network, Menlo Park, CA, USA

Summary

Sarcopenia and exercise intolerance are major contributors to reduced quality of life in the elderly for which there are few effective treatments. We tested whether enhancing mitochondrial function and reducing mitochondrial oxidant production with SS-31 (elamipretide) could restore redox balance and improve skeletal muscle function in aged mice. Young (5 mo) and aged (26 mo) female C57BL/6Nia mice were treated for 8-weeks with 3 mg/kg/day sS-31. Mitochondrial function was assessed *in vivo* using ^{31}P and optical spectroscopy. SS-31 reversed age-related decline in maximum mitochondrial ATP production (ATPmax) and coupling of oxidative phosphorylation (P/O). Despite the increased *in vivo* mitochondrial capacity, mitochondrial protein expression was either unchanged or reduced in the treated aged mice and respiration in permeabilized gastrocnemius (GAS) fibers was not different between the aged and aged+SS-31 mice. Treatment with SS-31 also restored redox homeostasis in the aged skeletal muscle. The glutathione redox status was more reduced and thiol redox proteomics indicated a robust reversal

All correspondence to: David J. Marcinek, South Lake Union Campus, 850 Republican St., Brotman D142, Box 358050, Seattle, WA 98109, (206) 221-6785, dmarc@uw.edu.

Author Contributions

M.D.C, J.V., M.J.M. W.J.Q. D.J.M. designed experiments; M.D.C, J.D, M.J.G., A.T.S, J.D.E. G.E.M., R.J.M., C.C.W. conducted experiments and collected data; M.D.C, L.W., T.K.B, T.J.K., H.H.S., P.S.R., M.J.M., W.J.Q., D.J.M. analyzed and interpreted data; and M.D.C. and D.J.M. wrote the manuscript.

of cysteine S-glutathionylation post-translational modifications across the skeletal muscle proteome. The gastrocnemius in the age+SS-31 mice was more fatigue resistant with significantly greater mass compared to aged controls. This contributed to a significant increase in treadmill endurance compared to both pretreatment and untreated control values. These results demonstrate that the shift of redox homeostasis due to mitochondrial oxidant production in aged muscle is a key factor in energetic defects and exercise intolerance. Treatment with SS-31 restores redox homeostasis, improves mitochondrial quality, and increases exercise tolerance without an increase in mitochondrial content. Since elamipretide is currently in clinical trials these results indicate it may have direct translational value for improving exercise tolerance and quality of life in the elderly.

Keywords

aging; fatigue; mitochondria; oxidative stress; skeletal muscle

Introduction

Sarcopenia, the age-related loss of skeletal muscle function, is a major contributor to the decline in the quality of life in the elderly for which there are few successful interventions. Age-related skeletal muscle degeneration, including both muscle atrophy and reduced performance of existing muscle, leads to exercise intolerance and is considered a key risk factor along the path to frailty, loss of independence, and poor quality of life. The associated costs were estimated to be 18 billion in the United States alone in 2000 and are expected to continue to increase due to the aging population [1]. Thus, there is a desperate need for interventions that will improve the quality of life for elderly individuals. Despite extensive effort there are few effective interventions, beyond exercise, that can prevent or restore skeletal muscle metabolic and contractile health in the elderly.

Mitochondria play a central role in skeletal muscle health. Sarcopenia is a complex pathology involving diverse age-related changes in metabolism and proteostasis, signaling pathways, chronic inflammation, disruption of neuromuscular junctions, and excitation-contraction defects [2]. However, mitochondrial dysfunction is involved in all of these processes as either a cause or consequence of these age-related changes. This central role of mitochondria in skeletal muscle health is due to their function as both the primary source of adenosine triphosphate (ATP) to meet the sustained energetic demand for muscle contraction and cell maintenance and their role as one of the main sources for cellular reactive oxygen species production. Reduced quality of mitochondria in aging skeletal muscle is manifested by a decline in ATP production accompanied by elevated oxidant production that disrupts both energy and redox homeostasis [3, 4].

Exercise tolerance and fatigue resistance depend on sustained ATP production by the mitochondria to fuel cross-bridge dynamics and calcium cycling that underlie muscle force production. Mitochondrial ATP production decreases with age in rodents and humans [5, 6]. When ATP or respiratory capacity is expressed per unit mitochondria there is a greater deficit [7, 8], indicating that both mitochondrial capacity and quality decline with age. Not

all studies have found a decrease in maximal mitochondrial ATP production in aging skeletal muscle [9], despite consistent agreement on the decline in exercise capacity and muscle health with age. In addition to their role in ATP production, mitochondria are also a significant source of superoxide from multiple sites within the electron transport system [10]. Thus, mitochondria are the main integrators of cell bioenergetics, redox biology, and cell signaling affecting muscle performance and health.

An important aspect of mitochondrial quality is the ability of mitochondria to produce ATP efficiently while minimizing oxidant production. Mitochondria from aged skeletal muscle produce elevated levels of superoxide and hydrogen peroxide [11] leading to increased redox stress. An important role for oxidative stress in muscle aging is supported by mice lacking Cu/Zn superoxide dismutase, which is found in the cytoplasm and inner mitochondrial space [12]. The absence of this enzyme results in elevated mitochondrial oxidant production and early development of sarcopenia due to the interaction between elevated mitochondrial oxidative stress in the neuromuscular junction and myofibers. Many studies have focused on oxidative damage to proteins, lipids, and DNA as the link between mitochondrial oxidative stress and tissue pathology, however, the concept of redox stress suggests that more subtle or reversible disruptions in redox signaling may play an important role in tissue pathology [13]. Increased redox stress can further inhibit mitochondrial ATP production and alter muscle contractility through direct effects on redox sensitive post-translational modifications (PTMs) on protein thiols [14, 15]. For example, a mild oxidative stress *in vivo* with low dose paraquat treatment induced energy deficits in Young mice that mimicked those observed with age. Additionally, mitochondrial energetics in old mice was more sensitive to this mild stressor [6]. These results are consistent with work demonstrating reversible inhibition of mitochondria in cells under redox stress [16]. Thus, elevated oxidant production due to poor mitochondrial quality in aged muscle can not only inhibit ATP production, but also contribute to sarcopenia through disruption of redox homeostasis and chronic activation of aberrant cell signaling.

The central role of mitochondria in skeletal muscle health points to direct manipulation of mitochondrial oxidative stress as a potential strategy to attenuate sarcopenia. We have previously shown that a single treatment with the mitochondrial targeted peptide SS-31 (elamipretide) improves mitochondrial coupling and maximal ATP production in aged mouse muscle [4]. SS-31 has also been shown to protect against mitochondrial related pathologies and injuries such as cardiac failure [17], disuse atrophy [18], Parkinson’s disease [19], ischemia-reperfusion injury [20] and severe burn trauma [21, 22]. The ability of SS-31 to target to the mitochondria [23] and associate with cardiolipin [24] while also enhancing ATP production [25] makes SS-31 an ideal therapeutic to test for long-term skeletal muscle health in aging tissue. In this study we test whether reducing mitochondrial oxidative stress with sustained treatment with SS-31 will lead to remodeling of the aged skeletal muscle resulting in functional improvement beyond those observed with a single acute treatment.

Results

SS-31 reverses energetic deficits in aged mitochondria

We delivered SS-31(3 mg/kg/day) or saline for 8 weeks to Young (5 mo) and old (26 mo) female mice using osmotic pumps. Simultaneous optical and ^{31}P magnetic resonance spectroscopy revealed that aging leads to decreased maximum ATP production (ATPmax) (Figure 1A) and coupling of oxidative phosphorylation (P/O ratio) (Figure 1B). Decline of *in vivo* P/O ratio in aged animals was largely driven by decreased ATPase activity rather than increased oxygen consumption with age (supplemental Figure 1A). The decline of mitochondrial function with age was further supported by a decreased energy state in aged skeletal muscle measured by resting phosphocreatine (PCr)/ATP ratio (Figure 1C) and ATP levels (Figure ID) and a resulting elevation of resting ADP levels (Table 1). Treatment with SS-31 reversed mitochondrial dysfunction in aged skeletal muscle resulting in increased ATPmax (Figure 1A), P/O ratio (Figure IB), and PCr/ATP (Figure 1C). Unexpectedly, resting ATP levels (Figure 1D) increased in the aged Ss-31 treated group. This change was not observed previously with acute treatment [4]. Treatment with SS-31 had no apparent effect on Young healthy muscle suggesting reversal of dysfunction rather than enhancement of mitochondrial *in vivo* bioenergetics by SS-31.

In order to differentiate between changes in mitochondrial capacity and mitochondrial quality we examined the effect of age and SS-31 treatment on markers of mitochondrial content and respiratory flux in homogenates and permeabilized muscle fibers (PMF) from the gastrocnemius muscle. Expression of protein subunits of the electron transport system (ETS) tended to be elevated in aged muscle relative to those of Young controls with a significant increase of complex III. In contrast to acute treatment, 8 weeks of SS-31 reversed this increase with significant differences in the expression of subunits of complexes I and III (Figure 1E and F). Only complex II appeared to be unaffected by age and SS-31 treatment. To further examine the effects of age and SS-31 on oxidative phosphorylation, we examined respiration in gastrocnemius PMF. PMF respiratory rates decreased with age in the presence of complex I substrates without ADP (LEAK), and in the presence of complex I and/or complex II substrates with 2.5mM ADP (state 3). PMF respiration was not affected by SS-31 (Figure 2A), and there were no significant effects of age or treatment on H_2O_2 flux (Figure 2B). Previous reports have shown that increased mitochondrial emission of H_2O_2 in aging mice is partially attenuated by SS-31 [26]. Examination of H_2O_2 production in gastrocnemius as a function of respiratory rate indicated that the aged ETS tended to be less efficient in the aged mitochondria under both leak and state 3 conditions. This trend was reversed, although not significantly following SS-31 treatment (Figure 2C and D). Analysis of the individual data points revealed a pattern where the variance in H_2O_2/O_2 was greater with age and reversed with SS-31 treatment due the presence of poor quality mitochondria in a subset of the aged mice. We measured mitochondrial content via citrate synthase activity and used this to normalize respiration and oxidant production. The decrease in respiration in the aged PMFs occurred despite an increase in citrate synthase activity (Figure 2E).

SS-31 improves redox homeostasis

Treatment with SS-31 has reduced mitochondrial oxidant production in multiple models [4,18, 27]. Therefore, we tested whether SS-31 rescue of mitochondrial deficits is associated with reduced oxidative damage and lower redox stress. 4-hydroxynonenal (HNE) modifications to proteins are markers of lipid peroxidation and were elevated in the aged gastrocnemius compared to Young. This age-related increase in oxidative damage was reversed by SS-31 (Figure 3A). To provide a snapshot of the redox status of the muscle we measured oxidized and reduced glutathione levels in the aged and aged+SS-31 mice. Free reduced glutathione (GSH) increased following SS-31 treatment without an accompanying effect on oxidized glutathione (GSSG) (Figure 3B) resulting in an elevated GSH/GSSG ratio indicative of a more reduced cell environment compared to the aged controls (Supplemental Figure 1B).

SS-31 interacts with cardiolipin (CL) in the mitochondrial membrane and preserves its interaction with components of the ETS [25]. Therefore, we assessed the effect of age and SS-31 on CL abundance and damage. This is particularly relevant because CL has been shown to be preferentially oxidized in certain disease states [28] and with age [29]. Mass spectrometry analyses of mature and monolyso-CL indicates effects of both age and SS-31 on CL. Contrary to previous reports in aging heart [29], there was no change in the abundance or isoform distribution of CL with age or treatment in gastrocnemius (Figure 3C and Supplemental Table 1). However, we observed an increase in the immature monolyso isoforms of CL (Figure 3D and Supplemental Table 1) with age that are partially reversed by SS-31 (Figure 3D). To assess potential changes in CL content per mitochondria as a measure of mitochondrial quality cardiolipin isoform abundance is normalized to citrate synthase to account for changes in mitochondrial content with age.

Both 8-week and acute treatment [4] with SS-31 show elevated GSH but what effect SS-31 and mitochondrial oxidant production has on redox sensitive post-translation modifications in aging skeletal muscle is unknown. For this reason, we assessed global cysteine protein S-glutathionylation, an important reversible oxidative PTM implicated in redox signaling [30], in Young, aged, and aged animals treated with SS-31 using a mass spectrometry based redox proteomics approach [31]. Increased S-glutathionylation with age was observed on a large number of cysteine residues and such increases were generally reversed by treatment with SS-31 (Figure 4A). Aged animals treated with SS-31 have a global profile of S-glutathionylation that differed from untreated aged animals and closely resembled Young animals. Protein cysteine residues with significant alterations of S-gluathionylation level (FDR<0.1) were sorted based on gene ontology (https://david.ncifcrf.gov/) and categorized by either biological function (Table 2) or cellular components (Table 3). Data for each ontology term was divided by the total number of gene products for each category to assess the percentage of proteins in each category with significantly altered S- glutathionylation. For this analysis, proteins with more than one modified cysteine residue were counted only once. The TCA cycle was the biological process with the highest percentage of proteins with significantly altered glutathionylation, nearly 50% in the case of the Age/Age+SS-31 comparison. This was followed by processes involved in sarcomeric structure and assembly (Table 2). Under the “cellular components” category, the mitochondria and sarcomere

structures were also represented among the top categories (Table 3). However, proteins involved in the interaction between the intracellular and extracellular environment appeared to be particularly susceptible to changes in redox status. Proteins associated with focal adhesion, the link between the plasma membrane and the extracellular matrix, and myelin sheath on motor neurons were highly modified in both comparisons indicating that the effect of mitochondria-induced redox perturbations extends well beyond the mitochondria into the extracellular environment. Although the glutathionylation state of only approximately 5% of the proteins in the overall mitochondria category were significantly altered by age or SS-31 treatment, the extent of significant alterations is greater when looking at sub-compartments of the mitochondria. Notably, age led to changes in modifications for approximately 10% of the proteins in the matrix and intermembrane space, while SS-31 treatment reduced S-glutathionylation of 13% and 18% percent of proteins in these categories, respectively.

Changes in protein S-glutathionylation may be explained by changes in fraction of the proteins oxidized or by changes in protein abundances. For this reason we assessed relative changes in protein abundance in parallel with S- glutathionylation proteomics. Despite numerous significant changes in S- glutathionylation levels there are relatively few significant changes in protein abundance either with age or treatment with SS-31 (Figure 4B). Using a threshold of FDR<0.1. Only 43 proteins were found to be significantly different comparing Young/Aged animals and no proteins were significantly different between Aged/Aged SS-31 treated animals. The top 5 pathways represented by these 43 proteins were identified by Ingenuity Pathway Analysis (IPA) (Qiagen Inc.) (supplemental table 2). To further verify that changes in S-glutathionylation are not caused by altered protein abundance we compared the fold-change in redox modification to that of protein abundance for cysteine residues significantly altered in both comparisons. There is no correlation between the datasets for either the Aged/Young or Aged/Aged SS-31 treatment (Figures 4C & D), r^2=0.004 and 0.007 respectively.

SS-31 improves skeletal muscle function

Following 8 weeks of SS-31 treatment, treadmill endurance was nearly doubled relative to untreated animals (Figure 5A). Running performance after 8 weeks of SS-31 was much greater than reported previously [4] after 8 days of treatment. Importantly, SS-31 treatment led to an approximate 30% increase in treadmill performance in aged animals compared to baseline (pre-treatment), whereas untreated aged animals actually decreased performance from baseline by approximately 20% (Supplemental Figure 1E). There was no effect in the Young mice. This indicates that the treatment not only prevented further decline in function during the 8-week period, but actually reversed some of the age-relate decline in exercise tolerance. Improved muscle performance was also reflected in increased *in situ* fatigue resistance measured in the tibialis anterior muscle using a maximal tetanic fatiguing protocol (Figure 5B). Despite improvement in fatigue resistance, SS-31 did not rescue age-related decline in specific force (Supplemental Figure 1F) and there was no apparent effect of aging or treatment on skeletal muscle gross morphology (data not shown) or muscle fiber size distribution (Supplemental Figure 1C) Despite the absence of an effect on fiber size, which is consistent with a previous report of treatment with SS-31 on aged muscle fiber size [26], there was a modest but significant protection of gastrocnemius muscle mass (Figure 5C) and

soleus (Table 4). However, the mass of the TA, EDL, and quadriceps were not significantly elevated following treatment (Table 4 & Supplemental Figure 1G).

Discussion

Directly targeting age-related mitochondrial dysfunction with the mitochondrial targeted peptide SS-31 improves skeletal muscle energetics and exercise tolerance. We have previously shown that acute SS-31 treatment improves *in vivo* bioenergetics and leads to increased skeletal muscle function in the form of greater treadmill endurance capacity and resistance to fatigue. [4]. This result led us to test the hypothesis that longer-term treatment would further improve mitochondrial quality and reverse age-related changes in skeletal muscle. We used a combination of *in vivo* NMR and optical spectroscopy to measure mitochondrial energetics in the mouse hindlimb. The decline in both ATPmax and P/O in the aged mice in this study is consistent with our previous work [4, 6] and *in vivo* energy deficits observed in aged human muscle using a similar approach [5, 32]. The reversal of age-related decline in ATPmax and P/O ratio *in vivo* observed after 8 weeks of SS-31 in this study is similar to that observed 1 hour after treatment [4], supporting a role for a rapidly reversible mechanism contributing to age-related mitochondrial deficits in skeletal muscle. Further support for this dynamic component to mitochondrial dysfunction in aging comes from work demonstrating that acutely increasing the mitochondrial oxidative stress in Young mice mimics age-related energy deficits [6]. However, in addition to improved bioenergetics, 8 weeks of SS-31 led to remodeling of the mitochondria ETS and increased resting ATP levels that were not observed with the acute treatment.

The improved *in vivo* energetics in aged mice treated with SS-31 was due to improved mitochondrial quality as measured by ATPmax, P/O, and PCr/ATP, and not the result of increased mitochondrial content. Loss of mitochondrial content and induction of mitochondrial biogenesis have received a lot of attention as potential targets for intervention to improve aging skeletal muscle [33]. However, we found that age-related *in vivo* mitochondrial deficits were independent of mitochondrial content in C57BL/6NIA mice. In fact, the trend of elevated expression of ETS subunits in aged muscle, despite mitochondrial energy deficits [6, 7], indicated that the decline in mitochondrial quality may be greater than indicated by the flux measurements alone. This reduced mitochondrial quality, i.e. reduced ATPmax per mitochondrial unit, has been observed in aged skeletal muscle in both humans [5] and mice [6] *in vivo* and *in vitro* in Fisher344BN rats [8]. Despite improvements observed for *in vivo* ATPmax and reduced oxidative stress there was no difference in state 3 respiration in PMF providing further evidence that improved *in vivo* ATPmax was not due to increased mitochondrial content. The elevation of reduced GSH and lower oxidative damage in treated aged muscle supports a model whereby the enhanced ETS function and reduced oxidative stress through treatment with SS-31 improves mitochondrial quality without relying on enhanced biogenesis or turnover.

We and others have previously identified an increase in mitochondrial H_2O_2 production by mitochondria from aged muscle [4]. In this previous work there was also an increase in variation within the aged group reflecting different rates of dysfunction or biological aging of the mitochondria. Although we did not observe a significant increase in the absolute

production of H_2O_2 by mitochondria in the aged group, the results from the current study are consistent with our previous results in that we observed greater ETS dysfunction, reflected by higher H_2O_2/O_2, in the mitochondria from aged muscle. Furthermore, the aged group reflected a range of biological aging of the mitochondria with 30–40% severely dysfunctional mitochondria. It is noteworthy that the SS-31 treated aged group lacked these severely dysfunctional mitochondria. This is consistent with other data from this study and our previous work [6] demonstrating that SS-31 has the greatest effect on poorly functioning mitochondria with little or no effect on healthy, high quality mitochondria. The repair of dysfunctional mitochondria was also consistent with the proposed mechanism whereby SS-31 stabilized the structure of oxidized cardiolipin to restore CL-protein interactions and membrane structure in damaged mitochondria [24].

One potential mechanism underlying improved mitochondrial quality following 8 weeks of SS-31 is a restoration of ETS protein assembly and stoichiometry. The increased abundance of some mitochondrial ETS proteins supports the hypothesis of a compensatory stimulation of mitochondrial biogenesis in the aged muscle and a loss of coordination between ETS proteins. A breakdown in coordination between the mitochondrial and nuclear encoded mitochondrial proteins has been observed in aged mouse muscles leading to mitochondrial dysfunction [34]. Restoration of this communication following treatment with nicotinamide mononucleotide (NMN) improves mitochondrial energetics. It is interesting to note that SS-31 restored the Young pattern of ETS protein expression, supporting the hypothesis that prolonged reduction of redox stress improves coordination of mitochondria protein expression and allows remodeling of the mitochondria in aged muscle. Poor assembly of the ETS proteins into functional complexes and supercomplexes provides another possible mechanism that could contribute to poor quality mitochondria. While the role of supercomplexes in mitochondrial function remains controversial, recent studies have demonstrated that changes in this structural organization can affect electron transport through the ETS [35] and that endurance training in elderly subjects increases supercomplex assembly and flux through the ETS [36]. This potential role for supercomplex structure is particularly interesting given the important role of the mitochondrial inner membrane phospholipid CL in assembly and stabilization of the ETS and inner mitochondrial membrane structure [37].

SS-31 preferentially interacts with CL on the inner mitochondrial membrane to stabilize its unique tetra-acyl structure during periods of elevated oxidative stress [25]. CL is required for maximal function of several components of the ETS, is essential for organization of respiratory supercomplexes, and anchors cytochrome c to the mitochondrial inner membrane [38]. Due to its high double-bond content, CL is prone to peroxidation during periods of oxidative stress [39]. Peroxidized CL is hydrolyzed by phospholipase A2 (PLA2) leading to degradation of CL and disruption of ETS function [40]. Alterations of CL content in skeletal muscle have been associated with increased lipid peroxidation [39], decreased ATP levels [41], and decreased complex IV activity [42] suggesting that disruption of CL content contributes to an increased oxidized mitochondrial environment increasing mitochondrial dysfunction. Addition of CL liposomes to rat heart following ischemia reperfusion (I/R) injury restores complex III activity [43], while addition of peroxidized CL did not rescue this activity indicating that the native structure of CL is required to support ETS function.

Treatment with SS-31 restored cardiac CL content in preclinical models of heart disease [44, 45]. Based on this previous work, we were surprised to observe no effect of age or SS-31 treatment on CL content in the mouse skeletal muscle. Because the monolyso form of CL, a three acyl chain intermediate CL species, is part of the metabolic cycle where CL is remodeled [39], changes in the abundance of these species indicates increased damage to CL. The increased ratio of mono-lyso CL to total CL in the aged muscle suggests an attempt to resynthesize CL with age. The reversal of this increased $MLCL/CL_{total}$ ratio in the SS-31 treated mice supports a preservation of CL structure by SS-31 that could improve the interaction and function among the components of the ETS and improve mitochondrial quality in aged skeletal muscle. Although the data cannot distinguish between a direct or indirect effect of SS-31 on CL, preservation of CL function by SS-31 treatment is consistent with reversal of expression levels of ETS complexes I, III, and IV, all of which are modified in CL deficiency [43, 46, 47].

Improved in vivo mitochondrial bioenergetics was associated with marked improvement in skeletal muscle function manifested as improved treadmill running and increased fatigue resistance in aged muscle treated with SS-31. We previously reported a small but significant increase in treadmill performance [4] after 8 days of daily SS-31 treatment. The current study demonstrates that 8-week treatment further improved exercise tolerance above baseline levels, Furthermore, when animals were tested at an intermediate time point of 4 weeks, the treated animals performed slightly better than their untreated counterparts but not to the level seen after 8 weeks of treatment (data not shown). Thus, longer periods of treatment lead to greater improvements in exercise tolerance despite the rapid increase of *in vivo* ATP generation [4]. The delay between rapidly increased ATPmax following acute treatment and gradually improved exercise tolerance over 8 weeks in this study indicates that mitochondrial ATP production cannot fully explain the functional improvements and suggests that restoration of redox and energy homeostasis lead to downstream changes to mitochondria and/or skeletal muscle to improve function. This was further supported by the small, but significant preservation of muscle mass in the gastrocnemius muscle in the aged +SS-31 group, something that is not observed with acute SS-31 treatment.

A causal relationship between mitochondrial oxidative stress and muscle performance is well established. Direct pharmacological manipulation of mitochondrial oxidative stress preserves or improves skeletal muscle performance in models of heart failure [48], disuse atrophy [18] and doxorubicin-induced toxicity [49]. Direct effects of oxidants on excitation-contraction coupling provides a link between mitochondria and muscle performance that is independent of ATP supply. Prolonged exposure to increased levels of H_2O_2 also decreases skeletal muscle force in muscle fibers from mice due to reduced myofibrillar Ca^{2}+ sensitivity that can be reversed through oxidant scavenging [50]. Disruption of redox homeostasis by mitochondrial H_2O_2 production results in oxidative modification of RyR receptors and calcium leak leading to muscle weakness and atrophy that is prevented by expression of the H_2O_2 scavenging enzyme catalase in the mitochondria [51]. Increased levels of ROS over time may also activate signaling proteolysis and apoptosis pathways. Activation of calpains, calcium dependent proteases, provides a mechanism linking mitochondrial oxidative stress, disruption of calcium homeostasis and loss of muscle mass [18, 49].

In addition to direct effects on aging and age-related pathology by oxidants, oxidative stress contribute to thiol-based redox modifications such as protein S-glutathionylation [52]. Decreased oxidative stress in aged animals by SS-31 has a profound effect on global S-glutathionylation. This effect is dramatic enough that the profile of glutathionylated proteins in aged animals treated with SS-31 looks more like a Young animal than an aged animal. Importantly this is not reflected in overall changes to protein abundance suggesting that altered S- glutathionylation is due to an increase in fraction of cysteine sites modified by glutathione. Pathway analysis of the few proteins whose abundance was significantly changed highlights stress response and myogenesis pathways, but the low number of changes in this assay limits the biological insights from this analysis. It should be noted that abundance proteomics approach reveals few target proteins that are altered with age or SS-31 treatment despite western blot analysis showing changes in electron transport proteins with age and rescue by treatment with SS-31. This is likely due to the increased statistical rigor of proteomics analysis.

The effect of increased S-glutathionylation on protein function is relatively poorly characterized. However, GO analysis indicated that age-related increases in mitochondrial redox stress can propagate throughout the cell. The high degree of modification of focal adhesion molecules near the plasma membrane and myelin sheath proteins surrounding the motor neuron suggests perturbation of the redox status of the extracellular environment. Reversal of these modifications by SS-31 treatment strongly supports an important role for mitochondrial redox biology in these modifications. Focal adhesion molecules play a role in linking the sarcolemma to the extracellular matrix, which is critical for formation and stabilization of the neuromuscular junction [53]. This is of particular interest given the growing recognition of the importance of loss of motor units and disruption of the neuromuscular junction in sarcopenia [54].

As expected, mitochondria were highly represented in the thiol redox proteomics results. Note that Tables 2 and 3 show data for GO categories ignoring multiple cysteine residues on the same protein. When not correcting for proteins with multiple cysteine residues, approximately 30% of all cysteine sites displaying significant alterations in S-gluathionylation were located in or associated with the mitochondria (459 of 1490 residues Aged/Young; 728 of 2691 residues Aged/Aged SS-31). However, given there are relatively few mitochondrial proteins, approximately 1100 [55], vs. approximately 20,000 proteins in the overall mammalian proteome [56], the fact that almost 30% of the significantly altered cysteine sites are mitochondrial suggests that spatial proximity to SS-31 may affect the glutathione system. While only 5% of mitochondria proteins were modified with age, it is important to note that this GO category includes over 5000 proteins, many of them with only a partial association with the mitochondria. Examination of the subcompartments of the mitochondria reveals that the matrix and intermembrane space were most affected by mitochondrial redox stress. These are the areas in closest proximity to production of superoxide at complex I and III sites of the ETS. It is interesting to speculate about whether the relatively greater effect of SS-31 treatment vs age on S-glutathionylation in the intermembrane space (18% vs. 9%) suggests that SS-31 has a preferential effect on superoxide produced in this compartment. We are focusing on protein S-glutathionylation level as an index of perturbation of redox status in the muscle cell. However, S-

glutathionylation also serves as a defense mechanism to protect against irreversible oxidative damage [52] and a regulatory mechanism in controlling protein function or activity. Previous work showing reversible S-glutathionylation is capable of regulating ETS complex I [57] as well as the F_1F_O ATPase function [58] suggests that reversal of redox stress by SS-31 may also operate through a mechanism of redox-sensitive PTMs in the electron transport system. It is these redox-sensitive PTMs that are typically lost during a normal mitochondrial isolation or permeabilized muscle fiber preparation that may account for the discrepancy between improved in vivo energetics and the lack of improvement in mitochondrial respiration reported here by treatment with SS-31. We propose that as muscle ages, mitochondrial dysfunction results in increased oxidative stress causing a shift of redox homeostasis and increased protein S-glutathionylation leading to a feedforward cycle, further disrupting both mitochondrial and contractile function of the muscle. SS-31 treatment for 8 weeks improves mitochondrial function, leading to restoration of redox homeostasis, thereby disrupting the feedforward cycle of dysfunction and ultimately restoring redox sensitive post-translational modifications and improved mitochondrial function.

In conclusion, this study showed that prolonged treatment with SS-31 reversed energetic deficits in aged mitochondria and improved resting and dynamic skeletal muscle function and redox homeostasis. Although increased mitochondrial ATPmax, restoration of redox homeostasis, restoration of redox - dependent post-translational modifications, and CL stabilization are discussed as distinct mechanisms, these processes are all linked through more efficient flux through the mitochondrial ETS and reduced mitochondrial oxidative stress. Benefits to mitochondrial structure, energetics and muscle performance after 8 weeks of treatment suggest that longer term intervention with SS-31 may further delay the effects of aging. The encouraging results in aging mouse muscle and the fact that SS-31 (elamipretide) is currently in human clinical trials demonstrates that targeting the mitochondria is a promising translational strategy for improving skeletal muscle function and increasing quality of life in the elderly.

Experimental Procedures

Animals

This study was reviewed and approved by the University of Washington Institutional Animal Care and Use Committee. Female C57BL/6 mice were received from the National Institute of Aging aged mouse colony. All mice were maintained at 21°C on a 14/10 light/dark cycle and given standard mouse chow and water *ad libitum* with no deviation prior to or after experimental procedures.

Surgery and SS-31

Osmotic minipumps (Alzet #1004) were loaded with isotonic saline or SS-31 in isotonic saline. sS-31 pumps were primed to deliver 3 $mg.kg^{-1}$/day. Animals were induced for anesthesia using 4% isoflurane in 1 L/min O_2 and maintained during surgery at 1.5–2% isoflurane on a circulating water pad at 37°C. An approximate 1 cm incision was made along the midline of the lower back, pumps were implanted subcutaneously, and the incision

was stapled shut using two 7 mm wound clips and dropped with Vetbond tissue glue (3M). Four weeks after initial surgery animals were anesthetized as before, pumps were removed and replaced with freshly filled and primed osmotic pumps.

In vivo spectroscopy and analysis

All tests were performed using a custom probe on a 14T vertical bore spectrometer (Bruker, Billerica, MA, USA). Mice were anesthetized by intraperitoneal injection of tribromethanol and the left hindlimb was shaved. Animals were suspended and their left leg was fixed into place inside a MR coil tuned to ^{31}P and ^{1}H. Fiber optic bundles ran along either side of the left leg to deliver light from a QTH source (Newport Corporation, Irvine, CA) and collect transmitted light by a CCD camera coupled to a spectrograph. A custom-fabricated inflatable cuff was positioned on the left hindlimb proximal to the MR coil and fiber optics bundles to allow blocking of blood flow and subsequent measurement of metabolites and myoglobin and hemoglobin saturation during experiments. Metabolite concentrations, and myoglobin and hemoglobin saturation levels were measured during fully relaxed (open-cuff) and fully ischemic states (inflated-cuff) as described in detail previously [59]. Optimization of MR signal was performed by shimming ^{1}H peak using water content of the hindlimb tissue and acquisition time was used to optimize optical signals. ^{31}P and optical spectra were acquired in parallel during fully relaxed (open-cuff) and ischemic states (inflated-cuff) and analysis was performed using MatLab custom scripts as previously described in detail [6].

Tissue preparation

A total of 5 cohorts were used allowing some tissues to be used for multiple purposes. All tissue was wet-weighed immediately following dissection. For histology left tibialis anterior was frozen in OCT for histology. For biochemistry gastrocnemius was flash-frozen in liquid nitrogen and stored at −80°C for extraction and measurement. For HPLC tibialis anterior was flash-frozen in liquid nitrogen and stored at −80°C for measurement of myoglobin, hemoglobin, and metabolites. For respirometry and H_2O_2 measurements a small section of gastrocnemius (~10 mg) was excised and permeabilized for immediate use. For CL content gastrocnemius was flash-frozen in liquid nitrogen and stored at −80°C for mass spectrometry.

Glutathione

Free reduced and oxidized glutathione were measured in gastrocnemius using the modified fluorescent-HPLC method developed by White et al [60], and described in detail previously [4].

Treadmill endurance

Mice were tested pre-surgery and after 8 weeks of treatment. Selected cohorts were also run at a 4-week timepoint. Mice were acclimated twice prior to each test. During all acclimation and tests a shock plate at the base of the treadmill was active delivering 0.15 amps at 1 Hz. On day one mice were placed on the treadmill at 0° incline allowed 2 minutes to free roam, then run for 2 minutes accelerating from 0 m/min to 10 m/min, and finally run for 2 minutes at 10 m/min. On day two mice underwent the same protocol with a maximum speed of 20

m/min. On test days mice were placed on the treadmill at 10° incline and exposed to a 5 min period accelerating from 0 m/min to 30 m/min, then run to exhaustion at 30 m/min. Exhaustion was noted as the inability to remount the treadmill after receiving 5 consecutive shocks and light physical prodding. All treadmill tests were run between 8 pm and 2 am to coincide with the natural active period of the mice.

In situ muscle mechanics and analysis

Animals were anesthetized and tested as previously described [4]. For fatigue tests tibialis anterior was stimulated through the peroneal nerve at 200Hz every other sec for 2 min. Specific force was measured using a single 200 Hz tetanic stimuli and normalized to cross sectional area of the tibialis anterior. Analysis was performed using Dynamic Muscle Analysis suite software (Aurora Scientific, Aurora, ON, Canada).

Metabolites, myoglobin, hemoglobin, and proteins

Creatine, ATP, and PCr concentrations in tibialis anterior was measured as previously described [59] using HPLC. Myoglobin and hemoglobin were measured in tibialis anterior by first separating proteins by SDS-PAGE followed by staining with Coomassie Brilliant Blue as previously described [59]. For protein extracts: snap frozen gastrocnemius was pulverized in CellLytic MT (Sigma C3228) with phosphatase and protease inhibitors using a bullet blender (Next Advance BBX24B) and centrifuge separated to remove cytoskeletal components. Protein extracts were separated using SDS-PAGE precast gels (Criterion #3450034). For Western blots: ETS complexes were blotted for measurement using a Total OXPHOS Rodent WB antibody cocktail (abcam #ab110413), HNE protein adducts were blotted for measurement using Anti-4 HNE (Alpha Diagnostic Intl. Inc. #HNE12-S)

Cardiolipin analysis

Individual muscle samples (approximately 10 mg) were homogenized in 600 μL of 10 times diluted PBS for 1 min (3 × 20 seconds with 10 seconds interval) at 4°C by using Precelleys Evolution homogenizer (Bertin Corp, MD). An aliquot of 25 μL was pipetted to determine the protein content (BCA protein assay kit, Thermo Scientific, Rockford, IL). The remaining homogenate was accurately transferred into a disposable glass culture test tube, and a mixture of lipid internal standards was added prior to lipid extraction for quantification of all reported lipid species and lipid extraction was performed by using a modified Bligh and Dyer procedure as described previously [61]. Each lipid extract was resuspended into a volume of 200 μL of chloroform/methanol (1:1, v/v) per mg of protein and flushed with nitrogen, capped, and stored at −20°C for lipid analysis. For shotgun lipidomics analysis of CL species, lipid extract was further diluted to a final concentration of ~500 fmol/μL, and the mass spectrometric analysis was performed on a QqQ mass spectrometer (Thermo TSQ QUANTIVA, San Jose, CA) and Orbitrap mass spectrometer (Thermo LTQ Velos, San Jose, CA) equipped with an automated nanospray device (TriVersa NanoMate, Advion Bioscience Ltd., Ithaca, NY) as previously described [62].

Ex vivo skeletal muscle respiration and H_2O_2 production

Approximately 10 mg of red medial gastrocnemius muscle was freshly dissected, separated, and permeabilized using saponin (50 μg/ml) at 4°C for 40 min. Fibers were placed in a 2 ml chamber of an Oxygraph 2K dual respirometer/fluorometer (Oroboros Instruments, Innsbruck, Austria) at 37°C and stirred gently during substrate and inhibitor titrations. Leak respiration was measured using malate (2 mM), pyruvate (5 mM), and glutamate (10 mM) prior to stimulation with ADP (2.5 mM) followed by succinate (10 mM) for State 3 respiration. Complex II respiration was measured using rotenone (0.5 μM) to inhibit complex I followed by complete mitochondrial respiration inhibition by antimycin A (2.5 μM). Finally, complex IV respiration was measured using TMPD (0.5 mM) and ascorbate (2 mM). H_2O_2 emission was measured in parallel with respiration using amplex red (50 μM) and HRP (0.1 U/ml).

Redox Proteomics analysis of S-glutahionylation

The redox proteomics experiments were performed as previously described for protein S-glutathionylation (P-SSG) [63–65]. Briefly, frozen mouse gastrocnemius muscles from SS-31 treated and untreated (saline vehicle) mice were minced while frozen and incubated for 30 min on ice in the dark in homogenization buffer comprised of 250 mM HEPES buffer pH 6.0,1% v/v SDS,1% v/v Triton X-100 and 100 mM n-ethyl-maleimide (NEM) to block all free thiols. A small portion of tissues were pooled from the untreated and treated samples, respectively, for total thiol profiling in which tissue was incubated in the same homogenization buffer without NEM. All tissue samples were then homogenized using a handheld homogenizer until completely homogenized. The resulting homogenate was pre-cleared by centrifugation at 14,000 rpm for 10 min at 4°C. The samples for P-SSG profiling were further incubated with 2 mM sodium ascorbate, 2 μM CuCl, and 1 mM SDS in the dark at 55°C for selective reduction of nitrosylated cysteine residues and complete alkylation of free thiols. The NEM blocking and ascorbate reduction step was omitted for the two total thiol profiling samples. All samples were then subjected to acetone precipitation overnight for complete removal of all excessive reagents such as detergents or NEM. Precipitated proteins were resuspended/solubilized in 250 mM HEPES buffer pH 7.0 containing 8 M urea and 0.1% SDS. Buffer exchange was performed twice using 250 mM HEPES buffer pH 7.0 containing 8 M urea, resulting in a final volume of 30–40 μL. Protein concentrations were measured by the BCA assay. Approximately 1mg of the protein solution was diluted to approximately 1 mL (~ 1 μg/μl) using 1 M urea in 25 mM HEPES buffer, pH 7.6 and then subjected to selective reduction of S- glutathionylated thiol residues using GRX1 enzyme cocktail containing 2.5 μg/mL GRX1M (C14S mutant from E. coli), 0.25 mM GSSG,1 mM NADPH, and 4 U/mL glutathionine reductase for P-SSG or reduced with 20 mM DTT in 25 mM HEPES buffer pH 7.7 containing 2% v/v SDS for 30 min at 37°C. Following the reduction step, free thiol-containing proteins were enriched using Thiopropyl Sepharose 6B resin with 564 μg protein per sample for SSG-channels and 250 μg protein per sample for total thiol. Following on-resin digestion, isobaric labeling with 10-plex tandem mass tag (TMT) reagents (Thermo Fisher Scientific) was performed. Briefly, 70 μL of anhydrous acetonitrile was added to the manufacturer-provided TMT reagent vials. Forty microliters of 100 mM triethylammonium bicarbonate (TEAB) buffer pH 8.5 and the 70 μL of the TMT reagent solutions were added to the resin containing peptides and the labeling reaction was

carried out at room temperature for 1 h. The reaction was stopped by the addition of 8 μL of 5% $NH_2OH{\cdot}HCl$ in 200 mM TEAB buffer for 15 min. The excess TMT reagents were removed by washing five times each with 80% ACN with 0.1% TFA and 25 mM ammonium bicarbonate. The captured, labeled peptides were eluted by DTT as previously described [31]. LC-MS/MS analysis was performed on an Q-Exactive plus mass spectrometer (Thermo Fisher Scientific) coupled with a Waters nanoACQUITY UPLC system. An MSGF plus algorithm was used to search MS/MS spectra against the mouse protein sequence database (UniProt, released in September 2016).

Abundance Proteomics

Protein Lysis and Digestion—Frozen tissue of 10–20 mg of mouse skeletal muscle was lysed with 0.5 mm zirconium oxide beads in 0.1% PPS (Expedeon) in 50 mM ammonium bicarbonate with 1X Halt phosphatase inhibitors (Pierce) in a Bullet Blender Storm homogenizer (Next Advance). Protein concentration was measured using a BCA protein assay (Pierce). Samples were reduced with DTT, alkylated with IAA and digested for 4 hours at 37 C with trypsin at an enzyme to substrate ratio of 1:50. Digests are acidified with 200 mM HCL and cleaned up with MCX columns (Waters). Pierce Peptide Retention Time Calibration (PRTC) mixture was added to each sample after digestion for downstream normalization.

Liquid Chromatography and Mass Spectrometry—A nanoACQUITY UPLC system (Waters Corporation) and Fusion Orbitrap mass spectrometer (Thermo Scientific) with an electrospray ionization (ESI) source was used. One ug of each digested sample and 150 femtomole of PRTC was loaded onto a 150 μm inner diameter Kasil (PQ Corporation) frit fused-silica microcapillary trap and 75 μm inner diameter column. Trap was packed with 3.5 cm of 3 μm Reprosil C18 reverse-phase material and the column was packed with 30 cm. PRTC was used to assess quality of the column before and during analysis. Four quality control runs were analyzed prior to any sample analysis and then after every six sample runs another quality control run was analyzed. The LC buffers were 0.1% formic acid in water (Buffer A) and 0.1% formic acid in acetonitrile (Buffer B). 60 minute gradient of the quality control consisted of 30 minutes of 98% buffer A and 2% buffer B, 5 minutes of 65% buffer A and 35% buffer B, 5 minutes of 40% buffer A and 60% buffer B, 7 minutes of 95% buffer A and 5% buffer B and 13 minutes of 98% buffer A and 2% buffer B at a flow rate of 0.3–0.35 μl/min.140 minute gradient for sample digest consisted of 90 minutes of 98% buffer A and 2% buffer B, 5 minutes of 65% buffer A and 35% buffer B, 5 minutes of 60% buffer A and 40% buffer B, 6 minutes of 5% buffer A and 95% buffer B and 34 minutes of 98% buffer A and 2% buffer B at a flow rate of 0.25 – 35 μl/min. Peptides were eluted from the column and electrosprayed directly into a QEHF mass spectrometer with application of a distal 2 kV spray voltage. For quality control analysis, a cycle of one full-scan mass spectrum (400–1600 m/z) with 120,000 resolution, AGC target of 5e6, 20 ms maximum injection time followed by 17 data-independent MS/MS spectra using an inclusion list at 15,000 resolution, AGC target of 5e5, 35 ms maximum injection time, 30% normalized collision energy with a 2 m/z isolation window. For sample digest, first a chromatogram library of 12 independent injections is analyzed from a pooled subset of samples. For each injection a cycle of one 60,000 resolution full-scan mass spectrum with a mass range of 50

m/z (400–450 m/z, 450–500 m/z…950–1000 m/z) followed by data-independent MS/MS spectra at 60,000 resolution, AGC target of 5e5,100 ms maximum injection time, 30% normalized collision energy with a 2 m/z isolation window. Chromatogram library data is used to quantify proteins from individual sample runs. Individual runs consist of a cycle of one 60,000 resolution full-scan mass spectrum with a mass range of **485–925** m/z, AGC target of **2e5**, 20 ms maximum injection time with profile data followed by data-independent MS/MS spectra at 30,000 resolution, AGC target of 1e5, 60 ms maximum injection time, 30% normalized collision energy with a 20 m/z isolation window. Application of the mass spectrometer and UPLC solvent gradients are controlled by the ThermoFisher XCalibur data system.

Data Analysis—Peptide identification and quantification follows a three-step process: 1)The narrow-window chromatogram library data (see Liquid Chromatography and Mass Spectrometry) data are searched using Pecan [66, 67] to generate a library of peptide detections consisting of elution times and MS/MS spectra for confident peptide detections. 2) PECAN-generated peptide library is used by EncycolopeDIA [68] to search the wide isolation window (20 *m/z*) data for each individual sample DIA LC-MS/MS run to generate a set of confident peptide detections in each of the runs and control the peptide false discovery rate on the experiment-wide level. 3) Skyline [69] is used to quantify the peptides identified by EncyclopeDIA and generate protein-level normalized intensity measurements used for relative protein quantification.

Chromatogram Library Generation

Chromatogram library data were searched using PECAN v. 0.9.9.2 in conjunction with a mouse proteome database (SwissProt) downloaded from Uniprot in October, 2014. Peptides with mass between 600 and 4000 Da and charge state +2 or +3 were included in the search space and the y-ion fragment series was used in the query. Only peptides clearing a 1% false discovery rate threshold were included in the library.

Library Search of Individual Sample Runs

Wide-window samples were acquired using an overlapping isolation window approach. The overlapping window data were demultiplexed and centroid using MSConvert (part of Proteowizard v3.0.10106) using overlap demultiplexing filter and vendor centroiding. Demultiplexed individual-sample LC-MS/MS DIA runs were queried using the library generated by PECAN. EncyclopeDIA v. 0.2.9.1 was used for this query with b and y-ions used for quantification, a 10 ppm precursor and fragment ion mass accuracy, and 5 quantitative ions used. The output of this analysis is an EncyclopeDIA library.

Protein Quantification using Skyline

EncyclopeDIA output consists of the following for each confidently identified (experiment-wide FDR < 0.01) peptide: the 5 optimal fragment ions to use for quantification, and the retention time boundaries (start and stop) bounding the peptide's chromatographic peak in each sample run. These values dictate which fragment ions are used for quantification of each peptide by Skyline as well as the retention time boundaries used for quantification. The demultiplexed individual sample runs were imported into Skyline-daily v. 3.6.1.10165 along

with the mouse proteome database which is used to map peptides to proteins. Each fragment ion was imported using a 10 ppm tolerance on the centroided *m/z*. Each individual sample run was normalized by the total ion current (TIC) extracted from the wide-window MS scans in each run. To generate protein-level intensity values, peptides mapping to multiple proteins in the protein database were discarded. For each protein, the integrated signal intensity (TIC normalized) from all confidently-identified peptides uniquely-mapping to the protein were summed to generate a protein-level measurement in each individual sample run.

Redox and Protein Intensity Heatmaps

In order to generate the heatmap, we computed a z-score of the log2-transformed intensity data, where we adjusted the data, by feature, to have a mean of zero and a standard deviation of 1. The heatmap is generated using the Complex Heatmap (v.1.17.1)R package [70], where both the samples and the features are clustered via the hclust function with the “complete” agglomeration method. Distance metric for clustering is computed using “Euclidean” distance. The heatmap in Figure 4A includes 2761 cysteine residues that were significantly different in either aged versus Young or aged versus aged+SS31 comparison at FDR of 0.1. The heatmap in Figure 4B includes 43 proteins that were significantly different in Young vs. aged saline comparison (FDR < 0.1).

Statistics

Statistical analysis was performed using Prism 6 software. Significance was determined using One-way ANOVA using Tukey correction for multiple comparisons or two-tailed students unpaired t-test as noted in figure legends. Levels of significance and sample sizes are also noted in figure legends.

Supplementary Material

Refer to Web version on PubMed Central for supplementary material.

Acknowledgments

Dr. David J. Marcinek has been a scientific advisor for Stealth BioTherapeutics. The authors would like to thank Rudy Stuppard for technical assistance with all aspects of this study and Xianlan Han, currently with the Barshop Institute for Longevity and Aging Research at UT Health San Antonio, and Quan He of the Sanford Burnham for analysis of CL isoform data. This work was supported by R21 AG042637, P01 AG001751,T32 AG000057, P30 ES007033, the University of Washington Nathan Shock Center (P30 AG013280) and the American Federation for Aging Research. Elamipretide (SS-31) was provided by Stealth BioTherapeutics, Inc.

References

[1]. Janssen, Shepard DS, Katzmarzyk PT, Roubenoff R, The healthcare costs of sarcopenia in the United States, J Am Geriatr Soc 52(1) (2004) 80–5. [PubMed: 14687319]

[2]. Marzetti E, Lees HA, Wohlgemuth SE, Leeuwenburgh C, Sarcopenia of aging: underlying cellular mechanisms and protection by calorie restriction, Biofactors 35(1) (2009) 28–35. [PubMed: 19319843]

[3]. Amara CE, Shankland EG, Jubrias SA, Marcinek DJ, Kushmerick MJ, Conley KE, Mild mitochondrial uncoupling impacts cellular aging in human muscles in vivo, Proc Natl Acad Sci U S A 104(3) (2007) 1057–62. [PubMed: 17215370]

[4]. Siegel MP, Kruse SE, Percival JM, Goh J, White CC, Hopkins HC, Kavanagh TJ, Szeto HH, Rabinovitch PS, Marcinek DJ, Mitochondrial-targeted peptide rapidly improves mitochondrial energetics and skeletal muscle performance in aged mice, Aging Cell 12(5) (2013) 763–71. [PubMed: 23692570]

[5]. Conley KE, Jubrias SA, Esselman PC, Oxidative capacity and ageing in human muscle, J Physiol 526 Pt 1(2000) 203–10. [PubMed: 10878112]

[6]. Siegel MP, Wilbur T, Mathis M, Shankland EG, Trieu A, Harper ME, Marcinek DJ, Impaired adaptability of in vivo mitochondrial energetics to acute oxidative insult in aged skeletal muscle, Mech Ageing Dev 133(9–10) (2012) 620–8. [PubMed: 22935551]

[7]. Kruse SE, Karunadharma PP, Basisty N, Johnson R, Beyer RP, MacCoss MJ, Rabinovitch PS, Marcinek DJ, Age modifies respiratory complex I and protein homeostasis in a muscle type-specific manner, Aging Cell 15(1) (2016) 89–99. [PubMed: 26498839]

[8]. Picard M, Ritchie D, Wright KJ, Romestaing C, Thomas MM, Rowan SL, Taivassalo T, Hepple RT, Mitochondrial functional impairment with aging is exaggerated in isolated mitochondria compared to permeabilized myofibers, Aging Cell 9(6) (2010) 1032–46. [PubMed: 20849523]

[9]. Kent-Braun JA, Ng AV, Skeletal muscle oxidative capacity in Young and older women and men, J Appl Physiol (1985) 89(3) (2000) 1072–8. [PubMed: 10956353]

[10]. Goncalves RL, Quinlan CL, Perevoshchikova IV, Hey-Mogensen M, Brand MD, Sites of superoxide and hydrogen peroxide production by muscle mitochondria assessed ex vivo under conditions mimicking rest and exercise, J Biol Chem 290(1) (2015) 209–27. [PubMed: 25389297]

[11]. Chabi B, Ljubicic V, Menzies KJ, Huang JH, Saleem A, Hood DA, Mitochondrial function and apoptotic susceptibility in aging skeletal muscle, Aging Cell 7(1) (2008) 2–12. [PubMed: 18028258]

[12]. Jang YC, Lustgarten MS, Liu Y, Muller FL, Bhattacharya A, Liang H, Salmon AB, Brooks SV, Larkin L, Hayworth CR, Richardson A, Van Remmen H, Increased superoxide in vivo accelerates age-associated muscle atrophy through mitochondrial dysfunction and neuromuscular junction degeneration, FASEB J 24(5) (2010) 1376–90. [PubMed: 20040516]

[13]. Sohal RS, Orr WC, The redox stress hypothesis of aging, Free Radic Biol Med 52(3) (2012) 539–555. [PubMed: 22080087]

[14]. Kramer PA, Duan J, Qian WJ, Marcinek DJ, The Measurement of Reversible Redox Dependent Post-translational Modifications and Their Regulation of Mitochondrial and Skeletal Muscle Function, Front Physiol 6 (2015) 347. [PubMed: 26635632]

[15]. Duan J, Gaffrey MJ, Qian WJ, Quantitative proteomic characterization of redox-dependent post-translational modifications on protein cysteines, Mol Biosyst 13(5) (2017) 816–829. [PubMed: 28357434]

[16]. Hill BG, Higdon AN, Dranka BP, Darley-Usmar VM, Regulation of vascular smooth muscle cell bioenergetic function by protein glutathiolation, Biochim Biophys Acta 1797(2) (2010) 285–95. [PubMed: 19925774]

[17]. Dai DF, Chen T, Szeto H, Nieves-Cintron M, Kutyavin V, Santana LF, Rabinovitch PS, Mitochondrial targeted antioxidant Peptide ameliorates hypertensive cardiomyopathy, J Am Coll Cardiol 58(1) (2011) 73–82. [PubMed: 21620606]

[18]. Min K, Smuder AJ, Kwon OS, Kavazis AN, Szeto HH, Powers SK, Mitochondrial-targeted antioxidants protect skeletal muscle against immobilization-induced muscle atrophy, J Appl Physiol (1985) 111(5) (2011) 1459–66. [PubMed: 21817113]

[19]. Yang L, Zhao K, Calingasan NY, Luo G, Szeto HH, Beal MF, Mitochondria targeted peptides protect against 1-methyl-4-phenyl-1,2,3,6-tetrahydropyridine neurotoxicity, Antioxid Redox Signal 11(9) (2009) 2095–104. [PubMed: 19203217]

[20]. Szeto HH, Liu S, Soong Y, Wu D, Darrah SF, Cheng FY, Zhao Z, Ganger M, Tow CY, Seshan SV, Mitochondria-targeted peptide accelerates ATP recovery and reduces ischemic kidney injury, J Am Soc Nephrol 22(6) (2011) 1041–52. [PubMed: 21546574]

[21]. Lee HY, Kaneki M, Andreas J, Tompkins RG, Martyn JA, Novel mitochondria-targeted antioxidant peptide ameliorates burn-induced apoptosis and endoplasmic reticulum stress in the skeletal muscle of mice, Shock 36(6) (2011) 580–5. [PubMed: 21937949]

[22]. Righi V, Constantinou C, Mintzopoulos D, Khan N, Mupparaju SP, Rahme LG, Swartz HM, Szeto HH, Tompkins RG, Tzika AA, Mitochondria-targeted antioxidant promotes recovery of skeletal muscle mitochondrial function after burn trauma assessed by in vivo 31P nuclear magnetic resonance and electron paramagnetic resonance spectroscopy, FASEB J 27(6) (2013) 2521–30. [PubMed: 23482635]

[23]. Zhao K, Zhao GM, Wu D, Soong Y, Birk AV, Schiller PW, Szeto HH, Cell-permeable peptide antioxidants targeted to inner mitochondrial membrane inhibit mitochondrial swelling, oxidative cell death, and reperfusion injury, J Biol Chem 279(33) (2004) 34682–90. [PubMed: 15178689]

[24]. Birk AV, Liu S, Soong Y, Mills W, Singh P, Warren JD, Seshan SV, Pardee JD, Szeto HH, The mitochondrial-targeted compound SS-31 reenergizes ischemic mitochondria by interacting with cardiolipin, J Am Soc Nephrol 24(8) (2013) 1250–61. [PubMed: 23813215]

[25]. Birk AV, Chao WM, Bracken C, Warren JD, Szeto HH, Targeting mitochondrial cardiolipin and the cytochrome c/cardiolipin complex to promote electron transport and optimize mitochondrial ATP synthesis, Br J Pharmacol 171(8) (2014) 2017–28. [PubMed: 24134698]

[26]. Sakellariou GK, Pearson T, Lightfoot AP, Nye GA, Wells N, Giakoumaki II, Vasilaki A, Griffiths RD, Jackson MJ, McArdle A, Mitochondrial ROS regulate oxidative damage and mitophagy but not age-related muscle fiber atrophy, Sci Rep 6 (2016) 33944. [PubMed: 27681159]

[27]. Anderson EJ, Lustig ME, Boyle KE, Woodlief TL, Kane DA, Lin CT, Price JW 3rd, Kang L, Rabinovitch PS, Szeto HH, Houmard JA, Cortright RN, Wasserman DH, Neufer PD, Mitochondrial H_2O_2 emission and cellular redox state link excess fat intake to insulin resistance in both rodents and humans, J Clin Invest 119(3) (2009) 573–81. [PubMed: 19188683]

[28]. Lokhmatikov AV, Voskoboynikova N, Cherepanov DA, Skulachev MV, Steinhoff HJ, Skulachev VP, Mulkidjanian AY, Impact of Antioxidants on Cardiolipin Oxidation in Liposomes: Why Mitochondrial Cardiolipin Serves as an Apoptotic Signal?, Oxid Med Cell Longev 2016 (2016) 8679469. [PubMed: 27313834]

[29]. Lesnefsky EJ, Minkler P, Hoppel CL, Enhanced modification of cardiolipin during ischemia in the aged heart, J Mol Cell Cardiol 46(6) (2009) 1008–15. [PubMed: 19303420]

[30]. Dalle-Donne I, Rossi R, Giustarini D, Colombo R, Milzani A, S- glutathionylation in protein redox regulation, Free Radic Biol Med 43(6) (2007) 883–98. [PubMed: 17697933]

[31]. Guo J, Gaffrey MJ, Su D, Liu T, Camp DG 2nd, Smith RD, Qian WJ, Resin-assisted enrichment of thiols as a general strategy for proteomic profiling of cysteine-based reversible modifications, Nat Protoc 9(1) (2014) 64–75. [PubMed: 24336471]

[32]. Conley KE, Esselman PC, Jubrias SA, Cress ME, Inglin B, Mogadam C, Schoene RB, Ageing, muscle properties and maximal O(2) uptake rate in humans, J Physiol 526 Pt 1(2000) 211–7. [PubMed: 10878113]

[33]. Vina J, Gomez-Cabrera MC, Borras C, Froio T, Sanchis-Gomar F, Martinez-Bello VE, Pallardo FV, Mitochondrial biogenesis in exercise and in ageing, Adv Drug Deliv Rev 61(14) (2009) 1369–74. [PubMed: 19716394]

[34]. Gomes AP, Price NL, Ling AJ, Moslehi JJ, Montgomery MK, Rajman L, White JP, Teodoro JS, Wrann CD, Hubbard BP, Mercken EM, Palmeira CM, de Cabo R, Rolo AP, Turner N, Bell EL, Sinclair DA, Declining NAD(+) induces a pseudohypoxic state disrupting nuclear-mitochondrial communication during aging, Cell 155(7) (2013) 1624–38. [PubMed: 24360282]

[35]. Lapuente-Brun E, Moreno-Loshuertos R, Acin-Perez R, Latorre-Pellicer A, Colas C, Balsa E, Perales-Clemente E, Quiros PM, Calvo E, Rodriguez-Hernandez MA, Navas P, Cruz R, Carracedo A, Lopez-Otin C, Perez-Martos A, Fernandez-Silva P, Fernandez-Vizarra E, Enriquez JA, Supercomplex assembly determines electron flux in the mitochondrial electron transport chain, Science 340(6140) (2013) 1567–70. [PubMed: 23812712]

[36]. Greggio C, Jha P, Kulkarni SS, Lagarrigue S, Broskey NT, Boutant M, Wang X, Conde Alonso S, Ofori E, Auwerx J, Canto C, Amati F, Enhanced Respiratory Chain Supercomplex Formation in Response to Exercise in Human Skeletal Muscle, Cell Metab 25(2) (2017) 301–311. [PubMed: 27916530]

[37]. Bazan S, Mileykovskaya E, Mallampalli VK, Heacock P, Sparagna GC, Dowhan W, Cardiolipin-dependent reconstitution of respiratory supercomplexes from purified Saccharomyces cerevisiae complexes III and IV, J Biol Chem 288(1) (2013) 401–11. [PubMed: 23172229]

[38]. Tuominen EK, Wallace CJ, Kinnunen PK, Phospholipid-cytochrome c interaction: evidence for the extended lipid anchorage, J Biol Chem 277(11) (2002) 8822–6. [PubMed: 11781329]

[39]. Chicco AJ, Sparagna GC, Role of cardiolipin alterations in mitochondrial dysfunction and disease, Am J Physiol Cell Physiol 292(1) (2007) C33–44. [PubMed: 16899548]

[40]. McLean LR, Hagaman KA, Davidson WS, Role of lipid structure in the activation of phospholipase A2 by peroxidized phospholipids, Lipids 28(6) (1993) 505–9. [PubMed: 8355576]

[41]. Santiago E, Lopez-Moratalla N, Segovia JF, Correlation between losses of mitochondrial ATPase activity and cardiolipin degradation, Biochem Biophys Res Commun 53(2) (1973) 439–45. [PubMed: 4268623]

[42]. Yamaoka S, Urade R, Kito M, Mitochondrial function in rats is affected by modification of membrane phospholipids with dietary sardine oil, J Nutr 118(3) (1988) 290–6. [PubMed: 3351630]

[43]. Petrosillo G, Ruggiero FM, Di Venosa N, Paradies G, Decreased complex III activity in mitochondria isolated from rat heart subjected to ischemia and reperfusion: role of reactive oxygen species and cardiolipin, FASEB J 17(6) (2003) 714–6. [PubMed: 12586737]

[44]. Eirin A, Ebrahimi B, Kwon SH, Fiala JA, Williams BJ, Woollard JR, He Q, Gupta RC, Sabbah HN, Prakash YS, Textor SC, Lerman A, Lerman LO, Restoration of Mitochondrial Cardiolipin Attenuates Cardiac Damage in Swine Renovascular Hypertension, J Am Heart Assoc 5(6) (2016).

[45]. Sabbah HN, Gupta RC, Kohli S, Wang M, Hachem S, Zhang K, Chronic Therapy With Elamipretide (MTP-131), a Novel Mitochondria-Targeting Peptide, Improves Left Ventricular and Mitochondrial Function in Dogs With Advanced Heart Failure, Circ Heart Fail 9(2) (2016) e002206. [PubMed: 26839394]

[46]. Paradies G, Petrosillo G, Pistolese M, Di Venosa N, Federici A, Ruggiero FM, Decrease in mitochondrial complex I activity in ischemic/reperfused rat heart: involvement of reactive oxygen species and cardiolipin, Circ Res 94(1) (2004) 53–9. [PubMed: 14656928]

[47]. Paradies G, Petrosillo G, Pistolese M, Di Venosa N, Serena D, Ruggiero FM, Lipid peroxidation and alterations to oxidative metabolism in mitochondria isolated from rat heart subjected to ischemia and reperfusion, Free Radic Biol Med 27(1–2) (1999) 42–50. [PubMed: 10443918]

[48]. Laitano O, Ahn B, Patel N, Coblentz PD, Smuder AJ, Yoo JK, Christou DD, Adhihetty PJ, Ferreira LF, Pharmacological targeting of mitochondrial reactive oxygen species counteracts diaphragm weakness in chronic heart failure, J Appl Physiol (1985) 120(7) (2016) 733–42. [PubMed: 26846552]

[49]. Min K, Kwon OS, Smuder AJ, Wiggs MP, Sollanek KJ, Christou DD, Yoo JK, Hwang MH, Szeto HH, Kavazis AN, Powers SK, Increased mitochondrial emission of reactive oxygen species and calpain activation are required for doxorubicin-induced cardiac and skeletal muscle myopathy, J Physiol 593(8) (2015) 2017–36. [PubMed: 25643692]

[50]. Moopanar TR, Allen DG, Reactive oxygen species reduce myofibrillar Ca2+ sensitivity in fatiguing mouse skeletal muscle at 37 degrees C, J Physiol 564(Pt 1)(2005) 189–99. [PubMed: 15718257]

[51]. Umanskaya A, Santulli G, Xie W, Andersson DC, Reiken SR, Marks AR, Genetically enhancing mitochondrial antioxidant activity improves muscle function in aging, Proc Natl Acad Sci U S A 111 (42) (2014)15250–5. [PubMed: 25288763]

[52]. Grek CL, Zhang J, Manevich Y, Townsend DM, Tew KD, Causes and consequences of cysteine S-glutathionylation, J Biol Chem 288(37) (2013) 26497–504. [PubMed: 23861399]

[53]. Li L, Xiong WC, Mei L, Neuromuscular Junction Formation, Aging, and Disorders, Annu Rev Physiol 80 (2018) 159–188. [PubMed: 29195055]

[54]. Rudolf R, Khan MM, Labeit S, Deschenes MR, Degeneration of neuromuscular junction in age and dystrophy, Front Aging Neurosci 6 (2014) 99. [PubMed: 24904412]

[55]. Ozawa T, Sako Y, Sato M, Kitamura T, Umezawa Y, A genetic approach to identifying mitochondrial proteins, Nat Biotechnol 21(3) (2003) 287–93. [PubMed: 12577068]

[56]. Clamp M, Fry B, Kamal M, Xie X, Cuff J, Lin MF, Kellis M, Lindblad-Toh K, Lander ES, Distinguishing protein-coding and noncoding genes in the human genome, Proc Natl Acad Sci U S A 104(49) (2007) 19428–33. [PubMed: 18040051]

[57]. Hurd TR, Requejo R, Filipovska A, Brown S, Prime TA, Robinson AJ, Fearnley IM, Murphy MP, Complex I within oxidatively stressed bovine heart mitochondria is glutathionylated on Cys-531 and Cys-704 of the 75-kDa subunit: potential role of CYS residues in decreasing oxidative damage, J Biol Chem 283(36) (2008) 24801–15. [PubMed: 18611857]

[58]. Garcia J, Han D, Sancheti H, Yap LP, Kaplowitz N, Cadenas E, Regulation of mitochondrial glutathione redox status and protein glutathionylation by respiratory substrates, J Biol Chem 285(51) (2010) 39646–54. [PubMed: 20937819]

[59]. Marcinek DJ, Schenkman KA, Ciesielski WA, Conley KE, Mitochondrial coupling in vivo in mouse skeletal muscle, Am J Physiol Cell Physiol 286(2) (2004) C457–63. [PubMed: 14522819]

[60]. White CC, Krejsa CJ, Eaton DL, Kavanagh TJ, HPLC-based assays for enzymes of glutathione biosynthesis, Curr Protoc Toxicol Chapter 6 (2001)

[61]. Wang M, Han X, Multidimensional mass spectrometry-based shotgun lipidomics, Methods Mol Biol 1198 (2014) 203–20. [PubMed: 25270931]

[62]. Han X, Yang K, Yang J, Cheng H, Gross RW, Shotgun lipidomics of cardiolipin molecular species in lipid extracts of biological samples, J Lipid Res 47(4) (2006) 864–79. [PubMed: 16449763]

[63]. Duan J, Kodali VK, Gaffrey MJ, Guo J, Chu RK, Camp DG, Smith RD, Thrall BD, Qian WJ, Quantitative Profiling of Protein S-Glutathionylation Reveals Redox-Dependent Regulation of Macrophage Function during Nanoparticle-Induced Oxidative Stress, ACS Nano 10(1) (2016) 524–38. [PubMed: 26700264]

[64]. Kramer PA, Duan J, Gaffrey MJ, Shukla AK, Wang L, Bammler TK, Qian WJ, Marcinek DJ, Fatiguing contractions increase protein S- glutathionylation occupancy in mouse skeletal muscle, Redox Biol 17 (2018) 367–376. [PubMed: 29857311]

[65]. Su D, Gaffrey MJ, Guo J, Hatchell KE, Chu RK, Clauss TR, Aldrich JT, Wu S, Purvine S, Camp DG, Smith RD, Thrall BD, Qian WJ, Proteomic identification and quantification of S-glutathionylation in mouse macrophages using resin-assisted enrichment and isobaric labeling, Free Radic Biol Med 67 (2014) 460–70. [PubMed: 24333276]

[66]. Ting YS, Egertson JD, Payne SH, Kim S, MacLean B, Kall L, Aebersold R, Smith RD, Noble WS, MacCoss MJ, Peptide-Centric Proteome Analysis: An Alternative Strategy for the Analysis of Tandem Mass Spectrometry Data, Mol Cell Proteomics 14(9) (2015) 2301–7. [PubMed: 26217018]

[67]. Ting YS, Egertson JD, Bollinger JG, Searle BC, Payne SH, Noble WS, MacCoss MJ, PECAN: library-free peptide detection for data-independent acquisition tandem mass spectrometry data, Nat Methods 14(9) (2017) 903–908. [PubMed: 28783153]

[68]. Searle BC, Pino LK, Egertson JD, Ting YS, Lawrence RT, MacLean BX, Villen J, MacCoss MJ, Chromatogram libraries improve peptide detection and quantification by data independent acquisition mass spectrometry, Nat Commun 9(1) (2018) 5128. [PubMed: 30510204]

[69]. MacLean B, Tomazela DM, Shulman N, Chambers M, Finney GL, Frewen B, Kern R, Tabb DL, Liebler DC, MacCoss MJ, Skyline: an open source document editor for creating and analyzing targeted proteomics experiments, Bioinformatics 26(7) (2010) 966–8. [PubMed: 20147306]

[70]. Gu Z, Eils R, Schlesner M, Complex heatmaps reveal patterns and correlations in multidimensional genomic data, Bioinformatics 32(18) (2016) 2847–9. [PubMed: 27207943]

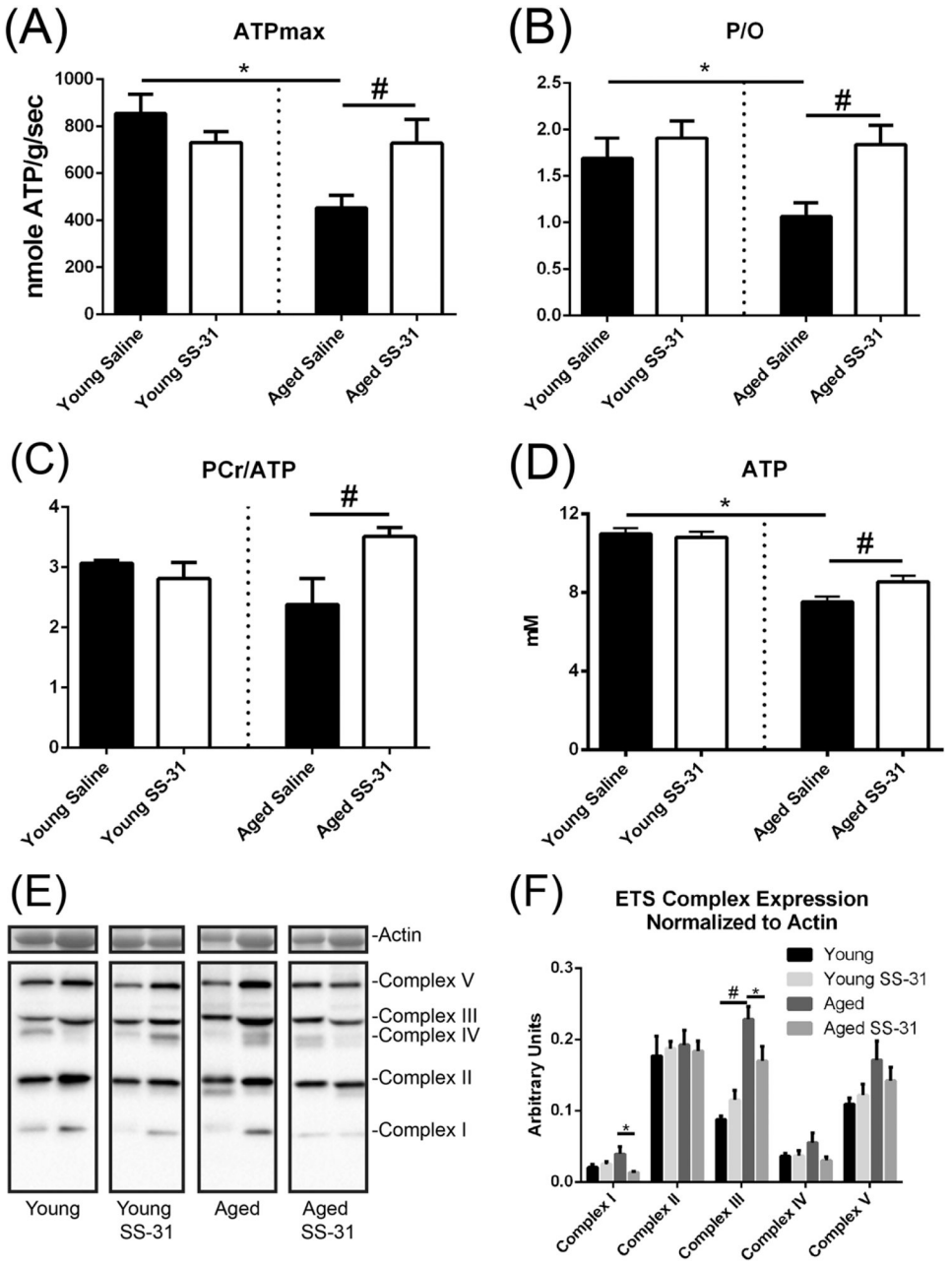

Figure 1. In vivo mitochondrial function and ETS expression

(A) ATPmax is significantly decreased in aged mice and rescued by treatment with SS-31 for 8 weeks. **(B)** In vivo P/O ratio is also decreased in aged animals and increased following SS-31 treatment. **(C)** Resting ATP levels are depressed in aged muscle and partially recovered by treatment with SS-31. **(D)** PCr/ATP is significantly decreased with age and increased with SS-31. **(E)** Representative western blots of ETS complex expression from each treatment group. Contrast has been turned up equally across all lanes for better visualization of some bands. **(F)** Quantification of ETS complex expression normalized to protein loaded. Complex III expression is increased with age and complexes I and III expression are decreased by SS-31. Data expressed as means ± SE, **(A-D)** student's unpaired

t-test, **(F)** One-way ANOVA $p<0.05$, n=7–9, *-significance compared to Young, #-significance compared to aged saline treated

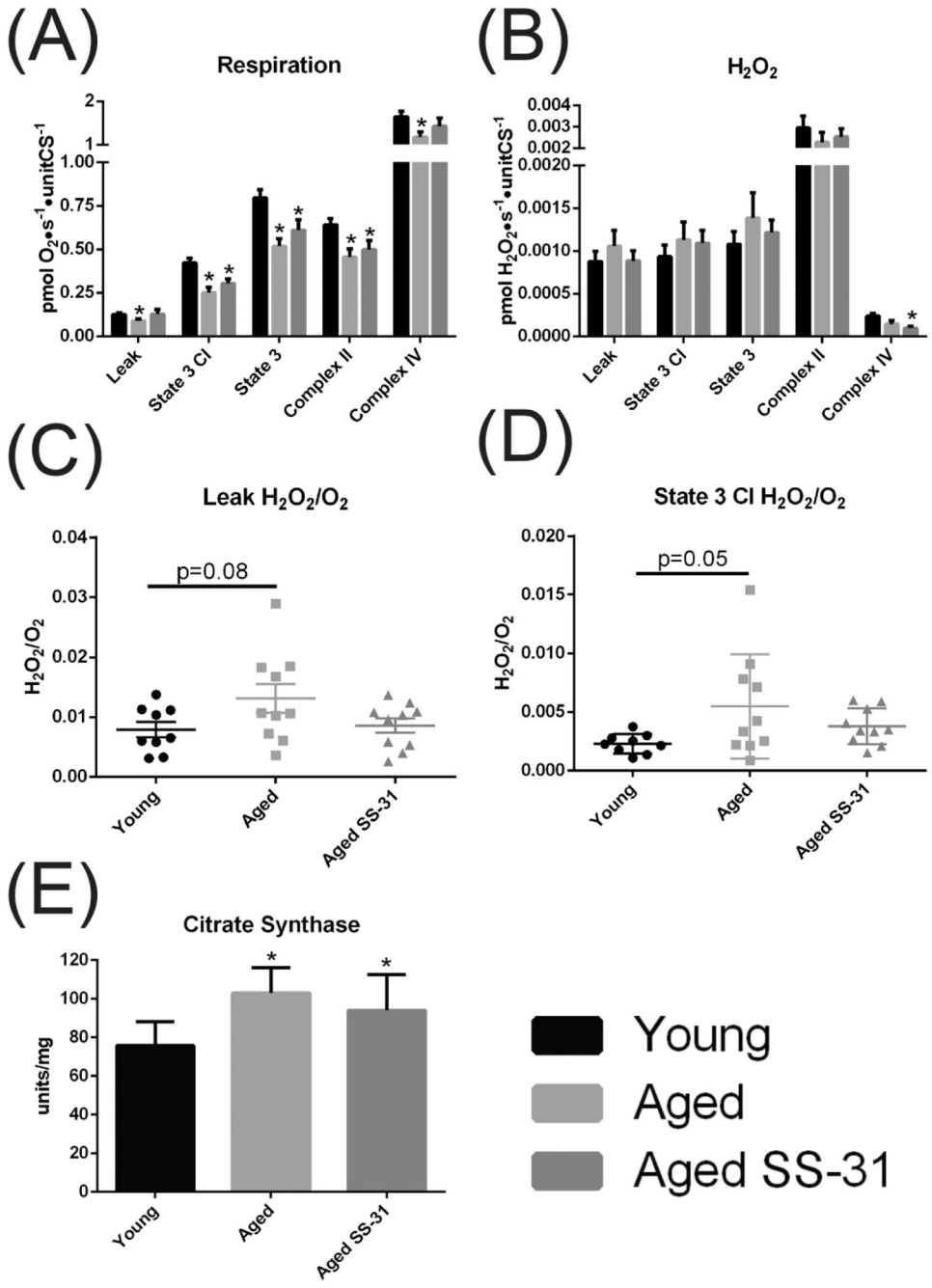

Figure 2. Ex vivo permeabilized fiber respiration and H_2O_2 production

(A) Oxygen consumption of permeabilized red gastrocnemius fibers. **(B)** H_2O_2 emission of permeablized gastrocnemius fibers. Respiration and H_2O_2 are expressed per unit CS activity. **(C)** H_2O_2/O_2 during leak state respiration **(D)** H_2O_2/O_2 during state 3 respiration using only complex I substrates plus 2.5mM ADP. **(F)** Citrate synthase activity. All data expressed as means ± SE, **(A-F)** student's unpaired t-test $p<0.05$, n=10, *-significance compared to Young, #-significance compared to aged saline treated

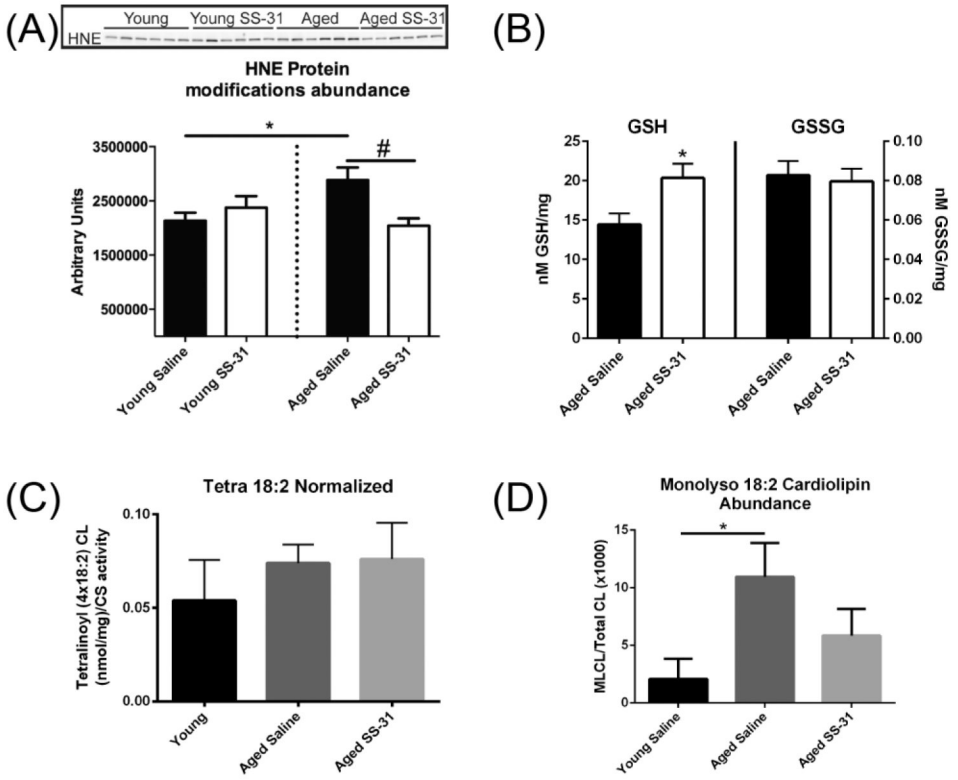

Figure 3. Redox state and cardiolipin expression

(A) Representative protein bands containing HNE protein adducts and quantification. HNE adducts increase with age and are decreased by treatment with SS-31. Contrast across all lanes has been adjusted equally for better visualization. Data expressed as means ± SE, $p<0.05$, n=7–9 **(B)** gSh is increased with SS-31 with no measurable effect on GSSG. Data expressed as means ± SE, $p<0.05$, n=6. **(C)** Tetra 18:2 cardiolipin is unaffected by age or treatment with SS-31 when normalized to mitochondrial content by citrate synthase expression**. (D)** SS-31 decreases tetra 18:2 monolyso cardiolipin content in aged animal skeletal muscle. Data expressed as means ± SE, **(A-D)** One-way ANOVA $p<0.05$, n=5, *-significance compared to Young, #-significance compared to aged saline treated

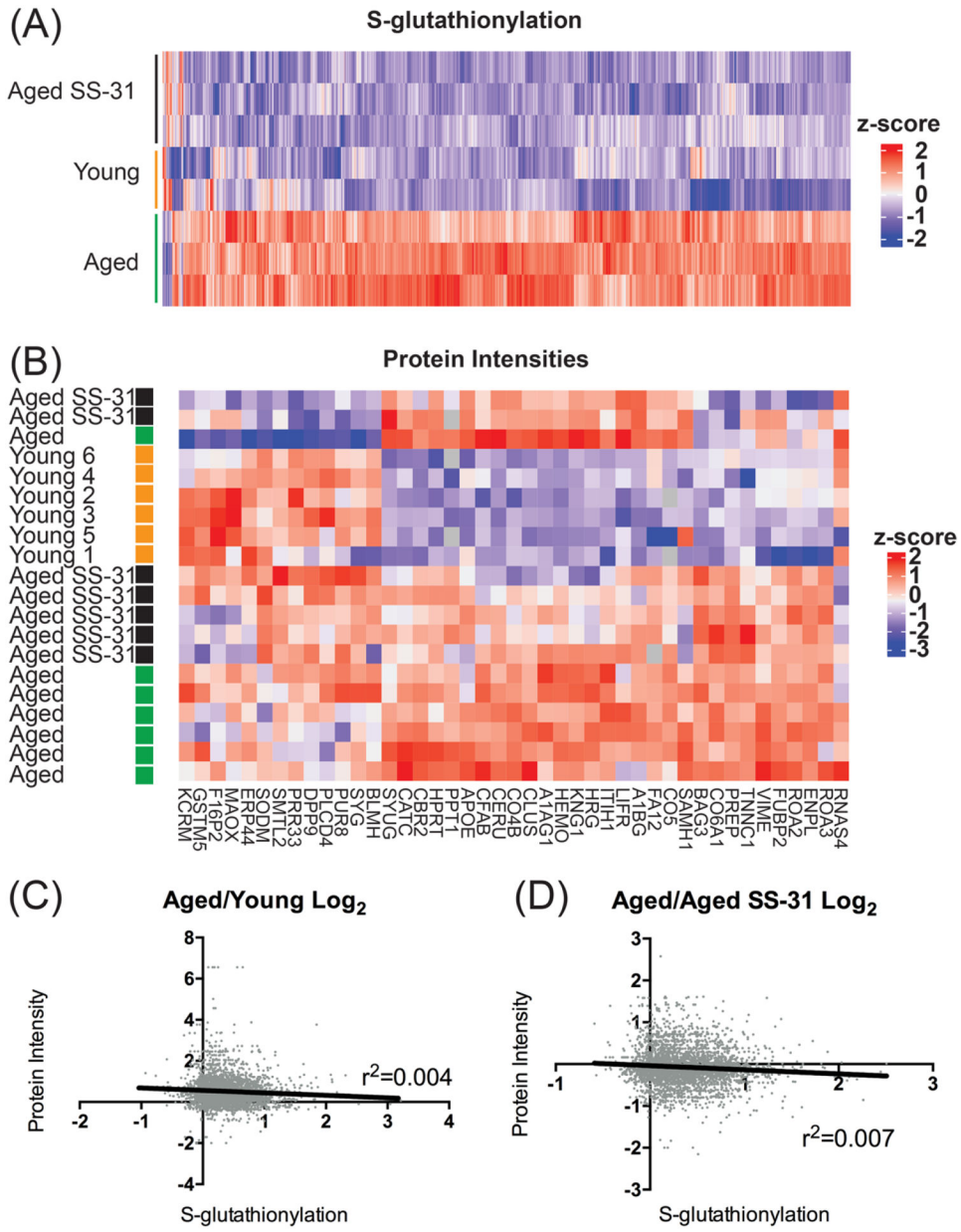

Figure 4. Global cysteine S-glutathione modifications and abundance proteomics.

(A) Protein S-glutationylation shows aged SS-31 cluster strongly with Young animals at the exclusion of aged untreated animals FDR<0.1.**(B)** Protein abundance proteomics shows no clustering of groups and very few proteins significantly altered with age with FDR<0.1. **(C&D)** Correlations of the Log_2 ratios in abundance and redox proteomics for Aged/Young and Aged/Aged- SS-31 comparison show no correlation between the two datasets.

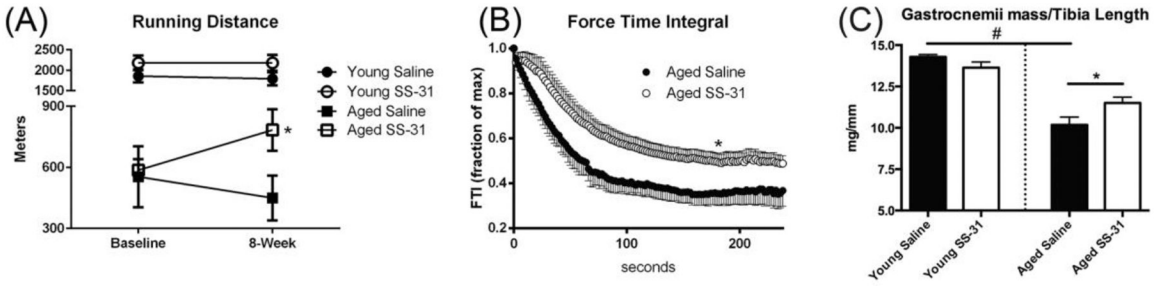

Figure 5. Muscle function and histology

(A) SS-31 increases treadmill performance in aged mice. Data expressed as means ± SE, $p<0.05$, n=5–7 mice. **(B)** SS-31 improves fatigue resistance in aged TA. Data expressed as means ± SE, $p<0.05$, n=7–8. **(C)** Sum of Left and right gastrocnemius normalized to tibia length. SS-31 partially preserves muscle mass in aged mice. Data expressed as means ± SE, $p<0.05$, n=8–11. **(A-C)** student's unpaired t-test #-significance compared to Young, *-significance compared to aged saline treated.

Table 1.

Metabolites.

Data expressed as means ± SE, *-p<0.05 compared to Young Saline, ‡-p<0.05 compared to Aged Saline.

	Young		Aged	
	Saline	**SS-31**	**Saline**	**SS-31**
Body mass (g)	25.6 ± 0.3	25.6 ± 0.5	26.6 ±0.7	27.4 ± 0.4
Adenosine triphospate (mM)	11.1 ± 0.3	10.3 ± 0.6	7.0 ± 0.5*	8.3 ± 0.3‡
Phosphocreatine (mM)	34.2 ± 1.1	30.0 ± 3.3	17.8 ± 3.7*	29.2 ± 1.6‡
Inorqanic Phosphate (mM)	2.9 ± 0.5	2.2 ± 0.1	2.3 ± 0.3	2.9 ± 0.3
Adenosine diphosphate (μM)	9.0 ± 5.7	6.3 ± 10.0	69.0 ± 24.0*	24.0 ± 6.3
pH_{Rest}	7.12 ± 0.04	7.13 ± 0.03	7.20 ± 0.04	7.17 ± 0.03
Myoqlobin (Mb) (nMol g^{-1})	0.033 ± 0.004	0.029 ± 0.002	0.033 ± 0.006	0.036 ± 0.004
Hemoqlobin (nMol g^{-1})	0.058 ± 0.010	0.063 ± 0.011	0.048 ± 0.016	0.054 ± 0.007
Resting Mb saturation (%)	93.6 ± 0.7	95.1 ± 1.5	83.2 ± 2.6*	83.5 ± 3.6

Table 2.

Gene Ontology Biological Processes.

Data show the top biological processes affected by age and treatment with SS-31 as a percentage of all gene products for that category. Proteins with multiple modified cysteine residues are only counted once. Thiol sites were filtered according to FDR<0.1 for inclusion in analysis.

	Aged/Young					Aged/Aged SS-31				
Bioloqical Process	**# of Prot.**	**% of qene products**	**Log2 Ratio**	**Lower CI 95%**	**Upper CI 95%**	**# of prot.**	**% of qene products**	**Log2 Ratio**	**Lower CI 95%**	**Upper CI 95%**
TCA Cycle	16	37.2	0.754	0.5728	0.9352	20	46.5	0.5817	0.4357	0.7278
Striated muscle myosin thick filament assembly	4	36.4	0.5337	0.2257	0.8416	5	45.5	0.4465	0.2836	0.6095
Sarcomere orqanization	15	24.2	0.6317	0.4276	0.8358	18	29.0	0.6803	0.4259	0.9347
Positive requlation of transcription from RNA polymerase II promoter	24	15.9	0.6451	0.5296	0.7607	35	23.2	0.5451	0.4739	0.6163
Protein homo-tetramerization	14	13.7	0.6764	0.5043	0.5966	16	15.7	0.7542	0.5966	0.9118
Protein stabilization	23	10.2	0.6088	0.4950	0.7226	31	13.8	0.5027	0.4327	0.5727
Cardiac muscle fiber development	4	5.7	0.7518	0.4562	1.047	5	7.1	0.8560	0.2533	1.965
Skeletal muscle fiber development	4	4.7	0.7092	0.09327	1.512	6	7.1	0.5808	0.4312	0.7303
Response to hypoxia	9	2.7	0.7038	0.5302	0.8775	19	5.8	0.6015	0.4311	0.7718
Cardiac muscle contraction	4	2.7	0.5077	0.2745	0.7408	16	4.3	0.5798	0.2870	0.8725
Skeletal muscle contraction	4	2.5	0.5828	0.4496	0.7160	13	3.1	0.7131	0.3159	1.110

Table 3.

Gene Ontology Cellular Compartments.

Data show the top cellular compartments affected by age and treatment with SS-31 and the mitochondrion broken down by sub compartments as a percentage of all gene products for that category. Proteins with multiple modified cysteine residues are only counted once. Thiol sites were filtered according to FDR<0.1 for inclusion in analysis.

	Aged/Young					Aged/Aged SS-31				
Cellular compartment	**# of Prot.**	**% of qene products**	**Log2 Ratio**	**Lower CI 95%**	**Upper CI 95%**	**# of Prot.**	**% of qene products**	**Log2 Ratio**	**Lower CI 95%**	**Upper CI 95%**
Focal adhesion	73	32.6	0.5941	0.5306	0.6575	102	45.5	0.5416	0.4857	0.5974
Myelin sheath	73	25.9	0.6198	0.5549	0.6846	95	33.7	0.5761	0.5204	0.6317
M band	10	20.0	0.6872	0.3482	1.026	14	28.0	0.5131	0.4119	0.6143
Z disc	30	14.7	0.5459	0.4084	0.6834	43	21.1	0.5559	0.4391	0.6727
Mitochondrion	258	4.4	0.6833	0.6472	0.7195	361	6.2	0.6023	0.5708	0.6339
Mitochondrial outer membrane	28	6.9	0.6421	0.5284	0.7558	31	7.64	0.5931	0.3175	0.05702
Mitochondrial intermembrane space	9	9.3	0.6255	0.3898	0.8613	18	18.6	0.4169	0.2919	0.5418
Mitochondrial inner membrane	74	7.9	0.6928	0.6302	0.7554	103	11.1	0.6064	0.5452	0.6676
Mitochondrial matrix	44	9.4	0.7809	0.6679	0.8938	62	13.2	0.6407	0.5548	0.7267

Table 4.

Body, tibia, and muscle measurements.

Data expressed as means ± SE, *-p<0.05 compared to Young saline, ‡-p<0.05 compared to Aged Saline

	Young Saline	Young SS-31	Aged Saline	Aged SS-31
Body Mass (g)	26.3 ± 0.57	25.6 ± 0.53	26.5 ± 0.65	27.4 ± 0.30
Tibia Length (mm)	18.8 ± 0.28	18.6 ± 0.24	18.3 ± 0.25	18.5 ± 0.24
Gastrocnemius L+R (mg)	269.0 ± 3.01	253.1 ± 6.44	186.0 ± 7.77*	212.8 ± 4.75‡
Tibialis Anterior L+R (mg)	86.35 ± 1.24	84.5 ± 1.97	67.4 ± 3.19*	72.8 ± 2.03
EDL L+R (mg)	20.04 ± 0.19	20.0 ± 0.53	16.4 ± 0.65*	17.4 ± 0.46
Soleus L+R (mg)	15.7 ± 0.29	15.3 ± 0.34	13.3 ± 0.36*	14.3 ± 0.33‡